A series of crystalline organic polymer–inorganic hybrid material zinc-phosphonate-phosphates synthesized in the presence of templates for superior performance catalyst support

Jing Huang [a,*], Jiali Cai [b], Chang Ming Li [c,*], Xiang Kai Fu [d]

[a] Research Center for Advanced Computation, School of Physics and Chemistry, Xihua University, Chengdu 610039, PR China
[b] College of Rongchang, Southwest University, Chongqing 402460, PR China
[c] Institute for Clean Energy & Advanced Materials, Southwest University, Chongqing 400715, PR China
[d] College of Chemistry and Chemical Engineering, Southwest University, Chongqing 400715, PR China

ABSTRACT

New types of organic copolymer–inorganic hybrid material zinc-phosphonate-phosphates are prepared with amines as templates. Notably, crystalline samples are obtained not with traditional methods but with simple reactions. Moreover, the samples are provided with the potential application as superior performance catalyst supports.

© 2014 Elsevier B.V. All rights reserved.

1. Introduction

Since the first synthesis of aluminium phosphate zeolites in 1982 [1], considerable interests have been focused on various metal phosphate materials [2]. Metal phosphonates exhibit a variety of open frameworks such as layered and microporous structures [3]. Materials with open framework and microporous structures are expected to find their use as hybrid composite materials in electro-optical and sensing applications in the future [4]. Research in the field of zirconium phosphates and zirconium phosphonates is very intense, which have involved mainly adsorbent [5–7], inorganic ion exchangers [8,9], intercalation chemistry [10,11], sensor and proton conductivity [12] and catalysis [13–15]. Our group has devoted ourselves to these in the last decades. Zirconium oligostyrenylphosphonate-phosphate (ZSPP) and zirconium poly(styrene-phenylvinylphosphonate)-phosphate (ZPS-PVPA) were prepared and used as catalyst supports. The immobilized catalysts display higher conversions, enantioselectivities and reusabilities than those achieved with the homogeneous catalysts under the same reaction conditions [16–22]. In addition, zinc phosphates have been proven to be very versatile in the formation of organic–inorganic hybrid materials [23,24]. In this work, a series of new types of organic copolymer–inorganic hybrid material zinc phosphonate-phosphate are prepared in the presence of templates (Scheme 1). The question as to whether or not crystalline zinc-phosphonate-phosphate hybrid materials could also be synthesized without the appending of templates and the roles of the templates as well as the feasibility for the superior catalyst performance supports are all examined here.
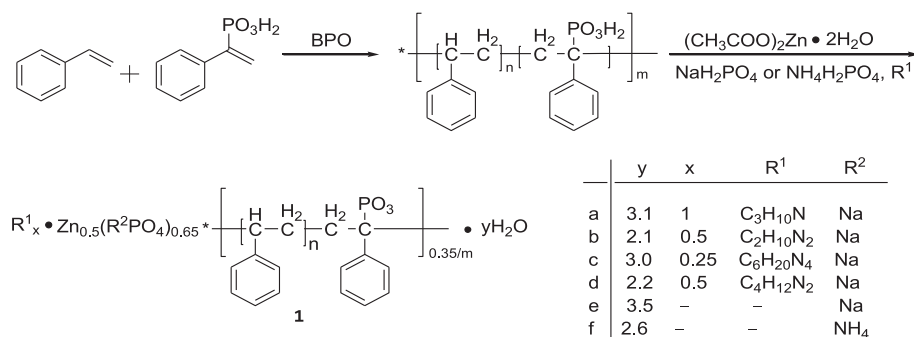
2. Results and discussion

The sodium content in sample 1e is 1.7%, which is 0.2% lower than that of theoretical values. This could be attributed to the surface-bound or intercalated water leading to the augment of the molecular weight.

According to FT-IR spectra (Fig. S1), the strong and wide absorption bands extending from 3100 to 3700 cm^{-1} and centering at 3500 cm^{-1} are assigned to the – OH, which verify the presence of H-bound interactions between the aminonium ion and pendant HPO_4^- group. The prominent bands at 1145, 1089, and 986 cm^{-1} are attributed to $R – PO_3^{2-}$ stretching vibrations. The absorptions at 1201, 1144, and 1077 cm^{-1} are due to the phosphonate and phosphate stretching vibrations.

On account of the TG curves (Fig. S2), samples 1a–1f lose 2.0–3.5 mol equivalents of surface-bound or intercalated water below 200 °C. There are two types of weight loss for these samples. According to samples 1a–1d, the surface-bound or intercalated water is firstly lost, followed by

* Corresponding authors.
   E-mail address: hj41012@163.com (J. Huang).

Scheme 1. Synthesis of **1**.

	y	x	R¹	R²
a	3.1	1	$C_3H_{10}N$	Na
b	2.1	0.5	$C_2H_{10}N_2$	Na
c	3.0	0.25	$C_6H_{20}N_4$	Na
d	2.2	0.5	$C_4H_{12}N_2$	Na
e	3.5	–	–	Na
f	2.6	–	–	NH_4

the decomposition of the templates, and then the sharp weight loss is in the temperature range of 200–600 °C, owing to the decomposition of the appended organic fragments. Finally, the small weight loss between 600 °C and 1000 °C is due to phase changes from layer to cubic $Zn_2P_2O_7$ and $NaZnPO_4$. While for samples **1e** and **1f**, the weight loss processes are similar to those of **1a–1d** apart from the absence of the decomposition of the templates. On the other hand, organic reactions are usually carried out below 200 °C. Therefore, the samples are provided with enough thermal stabilities as catalyst supports.

XRD patterns (Fig. S3) indicate that **1a–1f** are in crystalline states and could be served as mesoporous materials. Simultaneously, the interlayer distances of samples **1a–1f** are approximately 11 Å, which are broader than those of inorganic zinc phosphate $Zn_3(PO_4)_2$ (10.61 Å). It may be that the styrene-phenylvinylphosphonic acid copolymer chains in the samples make the zinc layer stretched and becoming broader. Moreover, pores or channels of various sizes and shapes are formed by appropriate modification of the styrene-phenylvinylphosphonic acid copolymer chain, further giving birth to a significant impact on the excellent catalytic activity. The interlayer distance of sample **1f** is a little narrower than that of the other samples, owing to the ammonium dihydrogen phosphate as the inorganic phosphate resource.

The diffuse reflectance UV–vis spectrums for samples **1a–1f** (Fig. S4) show a strong absorption around 227 nm, which may be assigned to the π–π* transition of the phenyl groups. Another strong absorption is shown around 326 nm. The phenomenon may be originated in two aspects of reasons. For samples **1a–1d**, this may be attributed to the involvement of the charge transfer transitions from the N atoms of the templates to the empty 4s orbitals of the Zn^{2+} ions, while for samples **1e** and **1f**, this perhaps is due to the O atoms of the phosphate or phosphonate to the empty 4s orbitals of the Zn^{2+} ions.

Based on the desorption isotherm (Fig. 1), sample **1c** indicates a hierarchical distribution of pore size. The pore diameters of the particles are mainly between 15 Å and 30 Å, and some other particles vary from 3 nm to 30 nm as well as few particles are over 30 nm in diameter.
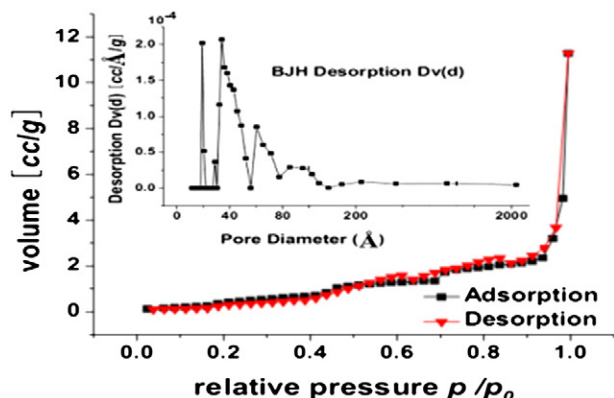
Meanwhile, the size of solvated Mn(salen)Cl complex is estimated to be 2.05–1.61 nm by MM2 based on the minimized energy [25]. On the basis of this, sample **1c** could provide enough room to accommodate the solvated chiral Mn(III) salen complex. In addition, the local environment inside the mesopores and pore size of the support definitely put effect on the enantioselectivity of the epoxidation. It is the crucial property that makes these samples being superior performance catalyst supports.

Compared with sample **1e**, different templates played different impacts on samples **1a–d** such as the physical properties of **1a–f** in Table 1.

In Fig. 2, the different morphologies of the samples are attributed to the templates and inorganic phosphate resources. As seen in sample **1a**, it is consisted irregularly of many platy layers, owing to the presence of the parts of zinc phosphonate in it. The anomalous clusters are induced by accumulation of the fraction of zinc phosphate in it. With regard to sample **1c**, the mixed powders of atypical particles and hexagonal bipyramid particles as well as anomalous suborbicular particles could be discerned, and for sample **1e**, there are regular neat plate layers which are mainly aggregation of the parts of zinc phosphate in it, while the anomalous roughly spherical segments are congregation of the proportion of zinc poly(styrene-phenylvinylphosphonate) in it. The appearances shed light not only on the intricate relationship among the open framework phosphates of different dimensionalities, but also on the mechanism of formation of the complex structures. Meanwhile, the supports possess various caves, holes, porous and channels. Some micropores and secondary channels would increase the surface area of the catalyst and provide enough chance for substrates to access to the catalytic active sites. While for sample **1f**, it is abnormally made up of lamellar sections and clusters. In a word, both various templates and different inorganic phosphate resources play vital impacts on the appearances of the samples and further influence the structure of the catalysts as well as the catalytic abilities.

TEM photographies of sample **1a** (Fig. 3) manifest that the configuration is filiform in structure and the sample consists of many irregular particles, while for sample **1e** (Fig. 4), the structure of the support is spheroid and their sizes are about 70–80 nm. The channels, holes and cavums could be observed clearly. Meanwhile, the average diameter of these secondary channels among the layers of the supports is around 50–60 nm. Based on the interlayer distance of the sample determined

Fig. 1. The nitrogen adsorption–desorption isotherm and pore distribution of sample **1c**.

Table 1
The physical properties of **1a–f**.

Sample	Surface area (m²/g)	Pore volume ($\times10^{-2}$ cm³/g)	Average pore diameter (nm)
1a	3.8	1.5	2.1
1b	4.6	1.8	3.1
1c	5.1	2.0	3.6
1d	4.4	1.9	3.3
1e	4.8	1.2	3.4
1f	4.9	1.3	3.5